Application of the Weierstrass Theorem for Sensors Signal Modelling

Plamen Nikovski, Tanya Titova, Nikolay Doychinov

University of Food Technologies, 26 Maritza Blvd., 4002 Plovdiv, Bulgaria

Abstract **– Modelling of sensor signals is a key element in implementing the procedures for estimation and tracking, sensor data fusion, fault detection and diagnosis, etc. In many cases, using traditional approaches to solve this problem is impossible due to lack of prior information about the observed process or particular sensor characteristics. Starting only from the finite rate of change of the signal at the output of real sensors, the Weierstrass theorem assumes the existence of a polynomial that approximates the signal, but does not specify how to find it. The present work attempts to solve this problem by assuming that the approximating polynomial has to retain that information in the signal which would allow its Bayesian estimation. The described approach has been successfully applied to model a humidity sensor signal, but it can be used in other cases without any problem.**

Keywords **– polynomial, model, sensor signals, approximation, Kalman filter, NIS.**

1. Introduction

A sensor is an element of a measurement system that is directly affected by the quantity associated with some physical phenomenon and the one that usually converts it into an electrical signal [1].

Actually, the sensor signal is a special kind of stochastic process. It can be defined as a set of real-valued sensor outcomes that occur in a successive order over time $\{f(t); t \in T\}$, where t represents the time and T is a subset of the time domain. Unfortunately, in many situations the function of the underlying data generation process $f(t)$ is unknown and this leads to problems. For example, an explicit mathematical description (model) of the output signal is a mandatory condition for implementing Kalman tracking algorithms [2-4], data fusion in multi-sensor systems [4-7], fault detection and diagnosis [8-10], etc. In such cases, we usually seek for a new function $p(t)$, simpler than $f(t)$, but close enough to it so that useful information from the measurements can be extracted by calculations performed on $p(t)$. The Weierstrass theorem [11] is fundamental to the success of this endeavor because it states that any continuous function can be approximated arbitrarily well by a polynomial. The theorem is simply defined as follows: It is assumed that $f(t)$ is a defined and continuous function of time in the finite interval $[t_0, t_1]$. Then for every $\varepsilon > 0$, there exists a polynomial with sufficiently high degree $(n-1)$

$$p(t) = a_{n-1}(t-t_0)^{n-1} + a_{n-2}(t-t_0)^{n-2} + \cdots + a_1(t-t_0) + a_0 \quad (1)$$

with the following property:

$$|f(t) - p(t)| < \varepsilon \quad (2)$$

for each $t \in [t_0, t_1]$. The coefficients of the polynomial $a_{n-1}, a_{n-2}, \ldots, a_0$ are real numbers, $a_{n-1} \neq 0$ and n is a natural number. Compared to other approximating functions, polynomials are well known, easy to define (a polynomial is completely defined by a finite set of coefficients) and fast to calculate by computer systems, which is important for real-time signal processing. In general, a more complex function $f(t)$, large intervals $[t_0, t_1]$ or small ε result in an approximating polynomial of higher degree [11] (some proofs and more information about the Weierstrass theorem can be found in [12,13]). In principle, the Weierstrass theorem allows the sensor signal to be written explicitly with some function (polynomial), but does not answer the question of how to do this. The present work aims to solve this problem.

DOI: 10.18421/TEM114-01
https://doi.org/10.18421/TEM114-01

Corresponding author: Plamen Nikovski,
University of Food Technologies, Bulgaria.
Email: plmnn@abv.bg

Received: 13 June 2022.
Revised: 01 August 2022.
Accepted: 03 August 2022.
Published: 25 November 2022.

2. State-space Polynomial Model

When trying to represent a polynomial in a state space [14] first of all the state variables have to be chosen. It is quite reasonable to use the value of the polynomial and its derivatives for this purpose:

$$\boldsymbol{x}(t) = (p(t) \quad \dot{p}(t) \quad \cdots \quad p^{(n-1)}(t))^T \tag{3}$$

where $x(t) \in \mathbb{R}^{n\times 1}$ is the state vector, $p^{(n)}$ is the n-th time-derivative of $p(t)$. Then the following continuous-time model is obtained immediately from (1):

$$\begin{aligned} \dot{\boldsymbol{x}}(t) &= \boldsymbol{A}\boldsymbol{x}(t) \\ p(t) &= \boldsymbol{C}\boldsymbol{x}(t) \end{aligned} \tag{4}$$

where the matrices

$$\boldsymbol{A} = \begin{pmatrix} 0 & 1 & 0 & \cdots & 0 \\ 0 & 0 & 1 & \cdots & 0 \\ \vdots & \vdots & \vdots & & \vdots \\ 0 & 0 & 0 & \cdots & 1 \\ 0 & 0 & 0 & \cdots & 0 \end{pmatrix} \tag{5}$$

$$\boldsymbol{C} = (1 \quad 0 \quad \cdots \quad 0),$$

$A \in \mathbb{R}^{n\times n}$ and $C \in \mathbb{R}^{1\times n}$. The first equation is known as a state equation and describes the evolution of the state variables, and the second equation known as the measurement equation determines the relationship between the value of the polynomial $p(t)$ and the state variables.

The components of the state vector can be obtained by differentiating expression (1):

$$\begin{aligned} x_i(t) &= p^{(i)}(t) \\ p^{(i)}(t) &= \sum_{j=i}^{n-1} \frac{j!}{(j-i)!} a_j t^{j-i}, i = 0, 1, \dots, n-1 \end{aligned} \tag{6}$$

Thus, for the variable $x_{n-1}(t)$ and its derivative it can be written:

$$\begin{aligned} x_{n-1}(t) &= (n-1)!\, a_{n-1} \\ \dot{x}_{n-1}(t) &= 0 \end{aligned} \tag{7}$$

The representations in the state space are not unique and if the state variables are chosen in a different way it is possible to obtain many other models equivalent to (4). The present model uses n state variables to describe a polynomial of degree $(n-1)$ and has an interesting property: the matrices A and C are known a priori and do not depend on the coefficients of the polynomial (coefficients a_j participate only in the state variables $x_i(t)$). The system (4) is a description in state space of all polynomials of degree $(n-1)$, and hence of those used for approximation in the Weierstrass theorem.

3. Discretization of a State-space Polynomial Model

The processes seen by sensors are often complicated, and even in a narrow time interval their signal cannot be expressed exactly with a polynomial. Thus, when a polynomial represents real signals, it is useful to have an element in the model which describes the discrepancy between them. A commonly applied technique to meet this requirement is the addition of process noise:

$$\begin{aligned} \dot{\boldsymbol{x}}(t) &= \boldsymbol{A}\boldsymbol{x}(t) + \boldsymbol{G}w(t) \\ y(t) &= \boldsymbol{C}\boldsymbol{x}(t) \end{aligned} \tag{8}$$

where $y(t)$ is the model output signal, process noise $w(t) \in \mathbb{R}$ is zero-mean white noise with covariance $E[w(t)w(t+\tau)] = q\delta(\tau), \quad q > 0$ is the noise intensity, $\delta(\tau)$ is a unit impulse function, $\boldsymbol{G} \in \mathbb{R}^{n\times 1}$ is a noise-driven matrix. In order to achieve a smoother signal at the model output and reduce the tuning parameters, it can be assumed that

$$\boldsymbol{G} = (0 \quad 0 \quad \cdots \quad 1) \tag{9}$$

which means that generally $x_{n-1}(t)$ does not remain constant but undergoes small unpredictable changes:

$$\begin{aligned} x_{n-1}(t) &\neq const \\ \dot{x}_{n-1}(t) &= w(t) \end{aligned} \tag{10}$$

Discretization of the model (8) is necessary since most numerical data processing procedures cannot use continuous-time process descriptions. In the discretization, the continuous model (8) is replaced by its discrete version

$$\begin{aligned} \boldsymbol{x}_{k+1} &= \boldsymbol{F}x_k + \boldsymbol{w}_k \\ y_k &= \boldsymbol{H}\boldsymbol{x}_k \end{aligned} \tag{11}$$

such that the outputs y_k and $y(t)$ of the two models coincide at time points $t_k = kT_s$, $k = 0, 1, 2, \dots$ (T_S is the sampling time that defines the interval between two adjacent observations):

$$y_k = y(kT)$$

The following equations are used to determine the discrete model parameters [15,16]:

$$\begin{aligned} \boldsymbol{F} &= e^{\boldsymbol{A}T_s} = \sum_{i=0}^{\infty} \frac{1}{i!} (\boldsymbol{A}T_s)^i \\ \boldsymbol{H} &= \boldsymbol{C} \end{aligned} \tag{12}$$

The discrete white noise $\boldsymbol{w}_k$ has zero mean and covariance matrix equal to $\boldsymbol{Q}\delta_{kl}$, respectively:

$$E\left[\boldsymbol{w}_k \boldsymbol{w}_l^T\right]_{T_s} = \boldsymbol{Q}\delta_{kl}, E[\boldsymbol{w}_k] = 0$$
$$\boldsymbol{Q} = q\int_0 e^{\boldsymbol{A}\tau}\,\boldsymbol{G}\boldsymbol{G}^T e^{\boldsymbol{A}^T\tau} d\tau \quad (13)$$
$$\delta_{kl} = \begin{cases} 0 \; if \; k \neq l \\ 1 \; if \; k = l \end{cases}$$

4. Low-order Polynomial Models of Signals

Discrete polynomial models of zero-, first- and second-order and their properties will be briefly discussed.

Zero-order polynomial model - When $(n-1) = 0$, it follows from (5), (6) and (8) that:

$$\dot{x}_1(\mathrm{t}) = 0 + w$$
$$y(t) = x_1 \quad (14)$$

A similar model describes a signal $y(t)$ whose value remains almost unchanged since its first derivative is white noise with zero mean. From (12) and (13) for the matrices of the discrete model it can be written:

$$\boldsymbol{F} = e^{\boldsymbol{A}T_s} = e^{0T_s} = \boldsymbol{I} = 1$$
$$\boldsymbol{H} = 1 \quad (15)$$
$$\boldsymbol{Q} = qT_s$$

First-order polynomial model - When $(n-1) = 1$, equations (5), (6) and (8) give:

$$\ddot{x}_1(\mathrm{t}) = 0 + w$$
$$y(t) = x_1 \quad (16)$$

A similar model describes a signal $y(t)$ whose rate of change remains almost unchanged as long as its second derivative is white noise with zero mean. From (12) and (13) for the matrices of the discrete model one can write:

$$\boldsymbol{F} = \begin{bmatrix} 1 & T_s \\ 0 & 1 \end{bmatrix}, \boldsymbol{H} = [1 \quad 0],$$
$$\boldsymbol{Q} = \begin{bmatrix} T_s^3/3 & \mathrm{T}_s^2/2 \\ \mathrm{T}_s^2/2 & T_s \end{bmatrix} q \quad (17)$$

Second-order polynomial model - When $(n-1) = 2$, equations (5), (6) and (8) yield

$$\dddot{x}_1(\mathrm{t}) = 0 + w$$
$$y(t) = x_1 \quad (18)$$

A model describes a signal whose acceleration remains almost unchanged (third derivative of $y(t)$ is a zero-mean white noise). From (12) and (13) it is not difficult to see that:

$$\boldsymbol{F} = \begin{bmatrix} 1 & T_s & T_s^2/2 \\ 0 & 1 & T_s \\ 0 & 0 & 1 \end{bmatrix}, \boldsymbol{H} = [1 \quad 0 \quad 0]$$
$$\boldsymbol{Q} = \begin{bmatrix} T_s^5/20 & T_s^4/8 & T_s^3/6 \\ T_s^4/8 & T_s^3/3 & T_s^2/2 \\ T_s^3/6 & T_s^2/2 & T_s \end{bmatrix} q \quad (19)$$

The models discussed above will be denoted by PM0, PM2 and PM3.

Measurements from real sensors always contain even small noise and this can also be taken into consideration:

$$\boldsymbol{x}_{k+1} = \boldsymbol{F}\boldsymbol{x}_k + \boldsymbol{w}_k$$
$$y_k = \boldsymbol{H}\boldsymbol{x}_k + v_k \quad (20)$$

where v_k is discrete zero-mean white noise with covariance matrix $E\left[v_k v_l^T\right] = R\delta_{kl}, R = r/T_s, r > 0$.

The system of equation (20) is a polynomial model of the sensor signal that will be used in this study.

5. Estimation of a Polynomial Model Parameters

Any polynomial model is uniquely described by three hyperparameters: the order of the polynomial model $(n-1)$ (the components of the matrices $\boldsymbol{F}$ and $\boldsymbol{H}$ are determined based on the order of the polynomial), the process noise intensity q, and the measurement noise intensity r. At this time, there is no general approach for their estimation, but when a polynomial model is used in Bayesian estimation procedures, the solution of such a problem is feasible [17].

Signal tracking usually refers to real-time estimation of certain signal parameters, e.g., minimum, maximum and mean values, rate of change, frequency, etc. The use of polynomial models as a process model in a Kalman filter is a highly efficient tool for estimating the expected value and covariance of a signal, two key features of importance to its post-processing and use.

Table 1. Kalman filter algorithm

Step 1	Define: model matrices $\boldsymbol{F}$ and $\boldsymbol{H}$; noise covariances $\boldsymbol{Q}$ and $\boldsymbol{R}$; initial state $\boldsymbol{x}_0$ and initial covariance $\boldsymbol{P}_o$.
Step 2	Predict state and covariance $\hat{\boldsymbol{x}}(k\|k-1) = \boldsymbol{F}\hat{\boldsymbol{x}}(k-1\|k-1)$ $\boldsymbol{P}(k\|k-1) = \boldsymbol{F}\boldsymbol{P}(k-1\|k-1)\boldsymbol{F}^T + \boldsymbol{Q}$
Step 3	Compute Kalman gain $\boldsymbol{K}(k) =$ $\boldsymbol{P}(k\|k-1)\boldsymbol{H}^T(\boldsymbol{H}\boldsymbol{P}(k\|k-1)\boldsymbol{H}^T + \boldsymbol{R})^{-1}$
Step 4	Correct state and covariance based on observation $\hat{\boldsymbol{x}}(k\|k) = \hat{\boldsymbol{x}}(k\|k-1)$ $+\boldsymbol{K}(k)(\boldsymbol{y}(k) - \boldsymbol{H}\hat{\boldsymbol{x}}(k\|k-1))$ $\boldsymbol{P}(k\|k) = (\boldsymbol{I} - \boldsymbol{K}(k)\boldsymbol{H})\boldsymbol{P}(k\|k-1)$
Step 5	Update the state and covariance values $\hat{\boldsymbol{x}}(k\|k-1) := \hat{\boldsymbol{x}}(k\|k)$ $\boldsymbol{P}(k\|k-1) := \boldsymbol{P}(k\|k)$ and go to Step 2

The Kalman filter is a form of Bayes filter that attempts to determine a posterior probability based on a priori information and a set of measurements [18-20]. For the model described by equations (20) the algorithm looks like the one given in Table 1.

Here it is assumed that the state $\boldsymbol{x}(k)$ is observed by m sensors which measurements together form the observation vector $\boldsymbol{y}(k) \in R^m$.

The Kalman filter is a recursive procedure, and therefore initial values of the state vector $\boldsymbol{x}_0$ and its covariance $\boldsymbol{P}_0$ need to be set at the start of the algorithm. When the system (20) is fully observable the error due to poor initialization decreases and usually tends to zero after the first few runs [21]. This gives some freedom to choose initial values.

If initialization in most cases does not have an effect on filter performance, the same cannot be said for hyperparameters. When the hyperparameters are well chosen the value $\boldsymbol{H}\hat{\boldsymbol{x}}(k|k-1)$ predicted by the model is close enough to the measured value $\boldsymbol{y}(k)$ and the innovation given by:

$$\boldsymbol{d}(k) = \boldsymbol{y}(k) - \boldsymbol{H}\hat{\boldsymbol{x}}(k|k-1) \tag{21}$$

is white Gaussian noise with zero mean and covariance $\boldsymbol{S}(k) = \boldsymbol{H}\boldsymbol{P}(k|k-1)\boldsymbol{H}^T + \boldsymbol{R}$:

$$\boldsymbol{d}(k) \sim N(0, \boldsymbol{S}(k)) \tag{22}$$

$$E[\boldsymbol{d}(k)\boldsymbol{d}(l)] = 0, \forall l \neq k \tag{23}$$

When condition (22) is satisfied, the scalar quantity

$$\gamma(k) = \boldsymbol{d}^T(k)\boldsymbol{S}^{-1}(k)\boldsymbol{d}(k) \tag{24}$$

known as normalized innovation squared (NIS) has a chi-squared distribution χ^2_m, with m degrees of freedom. Suppose that N independent observations of the sensor outputs at time k are obtained using a series of trials conducted under the same conditions and the values $\gamma_1(k), \gamma_2(k), \ldots, \gamma_N(k)$ are calculated for each of them. It is easy to prove that the sum:

$$\gamma(k) = \sum_{i=1}^{N} \gamma_i(k) \tag{25}$$

also has a chi-squared distribution, but with $m.N$ degrees of freedom [21]. When $\gamma(k)$ falls in the interval $Q_\gamma(\alpha/2) \leq \gamma \leq Q_\gamma(1-\alpha/2)$ where $Q_\gamma(\alpha/2)$ and $Q_\gamma(1-\alpha/2)$ are quantiles of order $\alpha/2$ and $(1-\alpha/2)$ of a chi-squared distribution with $m.N$ degrees of freedom, the hypothesis of fulfillment of the condition (22) can be accepted with probability $100(1-\alpha)$. Otherwise, the hypothesis and the chosen polynomial model are rejected.

If $d(k)$ is an arbitrary component of the vector $\boldsymbol{d}(k)$ and condition (23) is true, the normalized autocorrelation function

$$\frac{E[d(k)d(l)]}{\sqrt{E[d^2(k)]E[d^2(l)]}} \tag{26}$$

will be zero. Using N trials conducted under the same conditions, the innovations $d_1(k), d_2(k), \ldots, d_N(k)$ and the quantity

$$\rho(k,l) = \frac{\sum_{i=1}^{N} d_i(k)d_i(l)}{\sqrt{\sum_{i=1}^{N} d_i^2(k) \sum_{i=1}^{N} d_i^2(l)}} \tag{27}$$

which has a distribution close to Gaussian with zero mean and variance $1/N$ [21], are computed. When the quantity $\rho(k,l)$ falls in the interval $Q_\rho(\alpha/2) \leq \rho \leq Q_\rho(1-\alpha/2)$ where $Q_\rho(\alpha/2)$ and $Q_\rho(1-\alpha/2)$ are quantiles of order $\alpha/2$ and $(1-\alpha/2)$ of a Gaussian distribution with zero mean and variance $1/N$, the hypothesis of fulfillment of the condition (23) can be accepted with probability $100(1-\alpha)$. Otherwise, the hypothesis and the chosen polynomial model are rejected. The autocorrelation test must be applied to each component of the vector $\boldsymbol{d}(k)$.

When both tests are successful it is reasonable to expect that the model contains enough information about the sensor signal so that signal estimation (tracking) is possible.

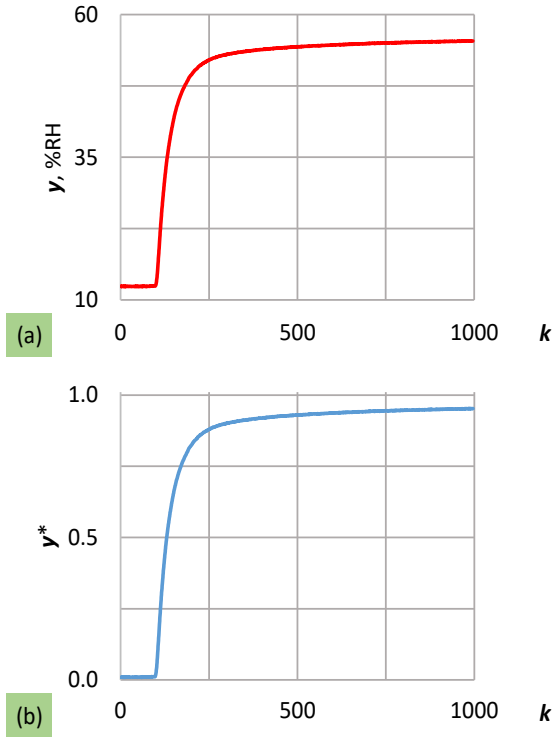

Figure 1. (a) Raw step response of the sensor when humidity increases. (b) Step response after normalization

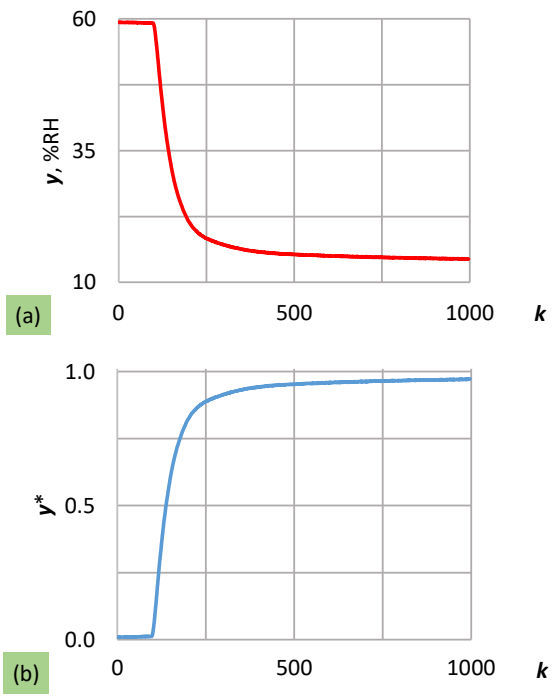

Figure 2. (a) Raw step response of the sensor when humidity decreases. (b) Step response after normalization

6. Polynomial Model of Humidity Sensor Signals

In order to find a polynomial model of the sensor signal we will use experimental data obtained by means of the data acquisition system described in [22]. The data include eight step responses of the SHT31-DIS humidity sensor. The first four recordings were made when the humidity increased stepwise from 12 %RH to 59 %RH, and the remaining four when it decreased stepwise from 59 %RH to 12 %RH. Each recording consists of 1000 discrete values taken at regular time intervals $T_s = 0{,}1\ s$. The data were normalized before being used:

$$y^*(k) = \frac{y(k) - y_{bi}}{y_{ei} - y_{bi}} \tag{28}$$

where y_{bi} and y_{ei} are the steady state output values before and after the start of the transient process, respectively. Figure 1 and Figure 2 show two of the obtained step responses before and after normalization.

The quantiles of the chi-square distribution and the Gaussian distribution defining the critical values for the two tests: $Q_\gamma\,(0{,}025) = 2{,}1797$, $Q_\gamma\,(0{,}975) = 17{,}5345$, $Q_\rho(0{,}025) = -0{,}6930$, $Q_\rho\,(0{,}975) = 0{,}6930$ are calculated for a significance level of $\alpha = 0{,}05$ and $N = 8$ degrees of freedom. For a fixed order polynomial, the noise intensities were chosen so that as many as possible values of γ and ρ fall within the acceptance regions.

The test results at $(n-1) = 0$ are presented graphically in Figure 3b-3f. The number of cases where γ falls in the rejection region is 192 out of 1000 (19,2 %). The resulting value exceeds the accepted significance level of 5 % many times, and the NIS test failed. We should immediately note that the bulk of the problem cases are at the beginning of the transient process where the rate of change of the sensor output is high. Towards the end of the transient process, there are almost no values outside the acceptance region.

The autocorrelation test is conducted at four different points ($k = 50{,}100{,}135$ and 600) for 50 consecutive readings ($l = k+1, k+2, \ldots, k+50$). It is noticed again that the test does not pass during the first part of the transient process (Figure 3d, 3e) where all 50 test values (100 %) fall in the rejection region.

The test results at $(n-1) = 1$ are shown in Figure 4b-4f. The number of cases in which γ falls within the rejection region is 54 out of 1000 (5,4 %). Even though the NIS test failed, the resulting value is very close to the threshold (the exceedance is only 0,4 %). The autocorrelation test failed only in the second case (Figure 4d), where the number of cases outside the acceptance region was 5 out of 50 (or 10%).

The test results of the second order polynomial model, $(n-1) = 2$ can be seen in Figure 5b-5f. The number of cases in which γ falls within the rejection regions is 36 out of 1000 (3,6 %), confirming that the NIS test passed. The number of ρ values outside the acceptance region does not exceed 2 out of 50 (2,5%) for all four cases (Figure 5c-5f), and the autocorrelation test is also successful. The results of the NIS test and the autocorrelation test suggest that a second-order polynomial model can be used to track the signals received from the sensor.

The zero- and first-order polynomial models are not able to fully track the signal received from the humidity sensor, but have the potential to handle cases where its dynamics is not high. This and their relative simplicity are sometimes sufficient reason to select and use them in solving certain problems.

Of the three models considered, only the second-order polynomial model allows the tracking of the sensor response under step changes in humidity. This is an important conclusion as it concerns the applicability of the model in the general case. When the dynamic system sensor - Kalman filter is linear and time invariant and the Kalman filter is able to track the sensor response for a step input (the innovation is zero-mean white noise), then according to the superposition principle the filter will be able to track the sensor response for any other input signal [17].

7. Conclusion

The rate of change of signals obtained from real sensors is always finite and therefore they can be described by a continuous real-valued function.

In these cases, the Weierstrass theorem allows the signal to be approximated by a polynomial, but does not say how to do this.

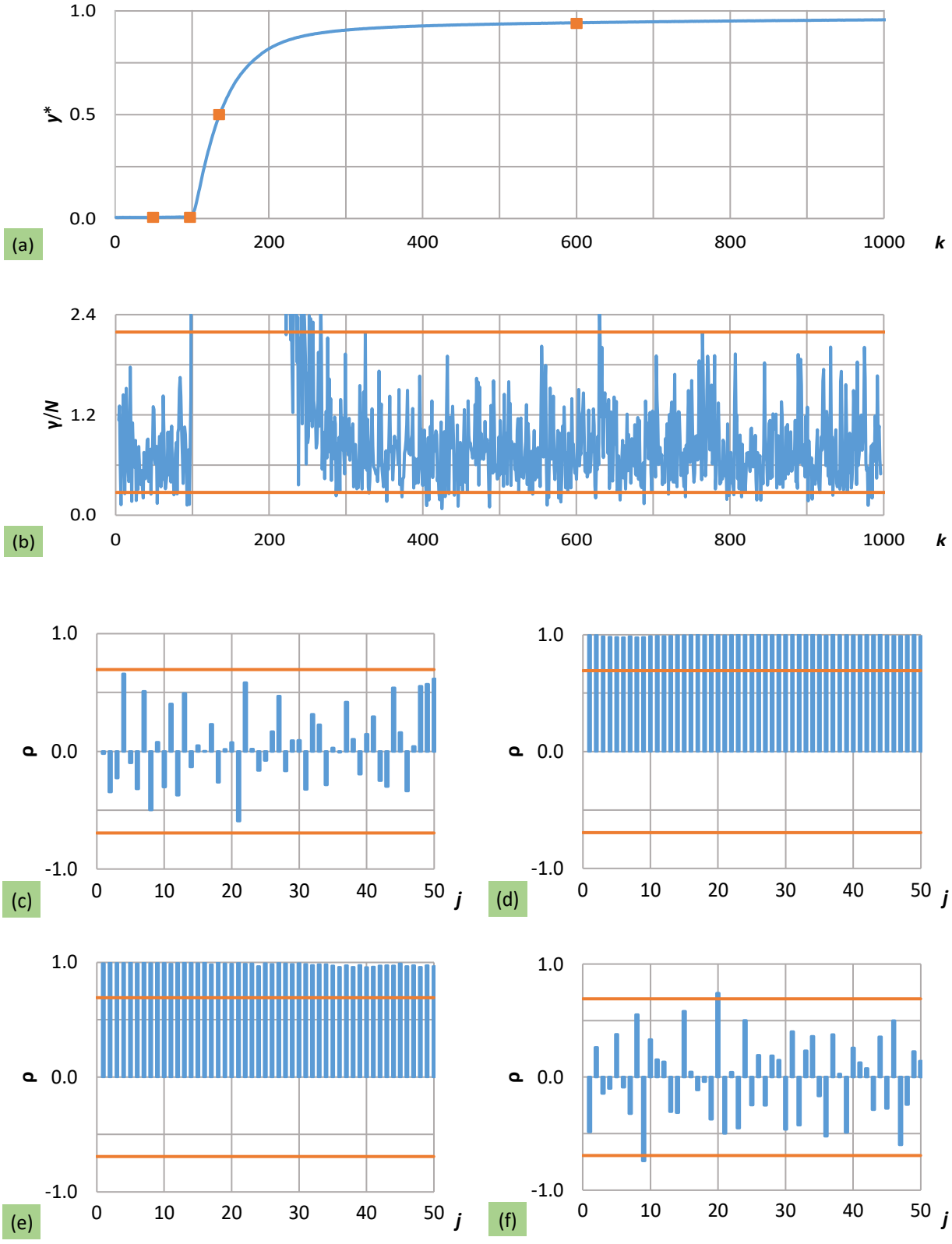

Figure 3. Zero-order polynomial model. (a) Mean of normalized sensor step response. (b) Normalized innovation squared test. (c)-(f) Autocorrelation test for different points of the transient response.

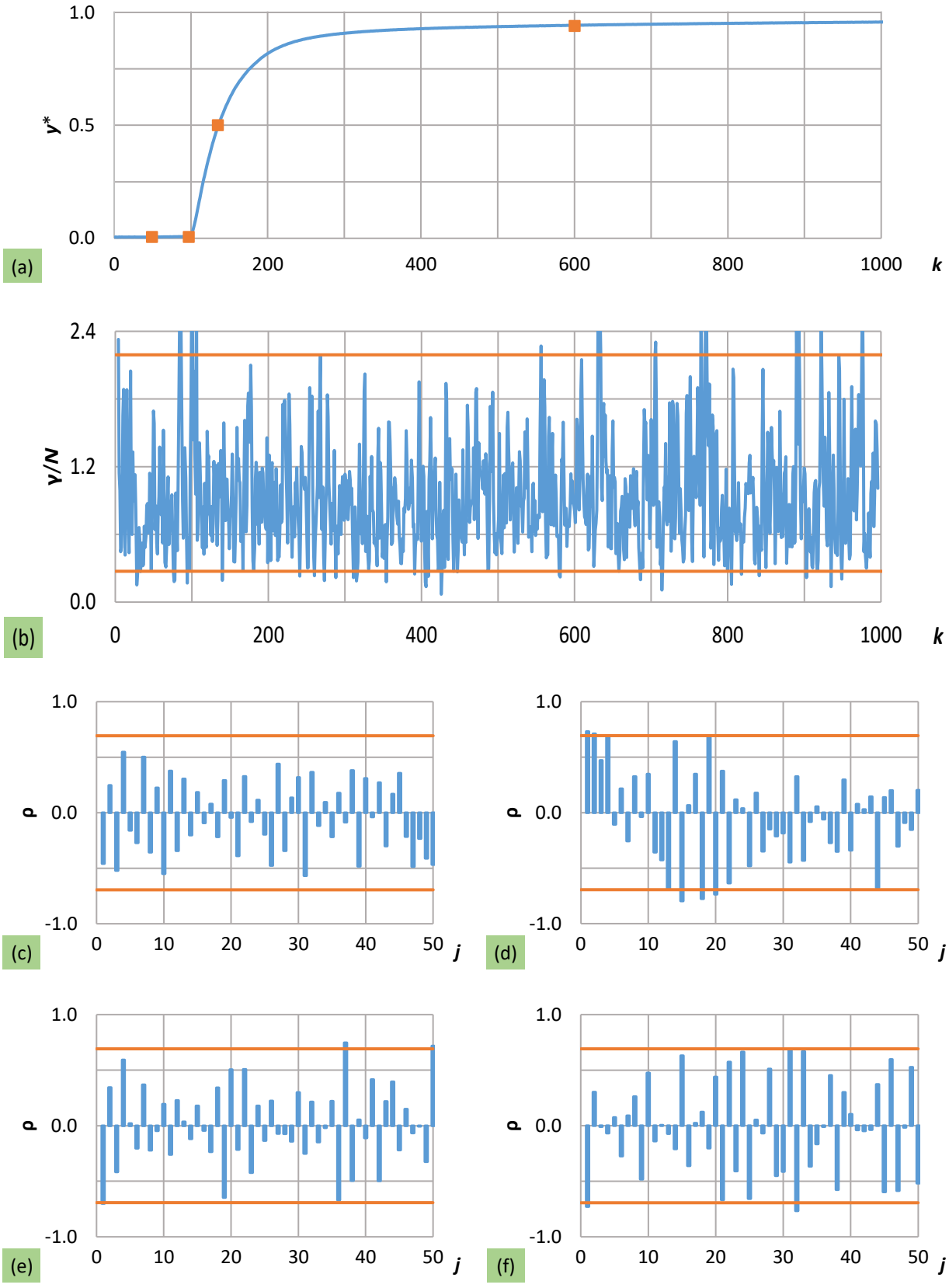

Figure 4. First-order polynomial model. (a) Mean of normalized sensor step response. (b) Normalized innovation squared test. (c)-(f) Autocorrelation test for different points of the transient response.

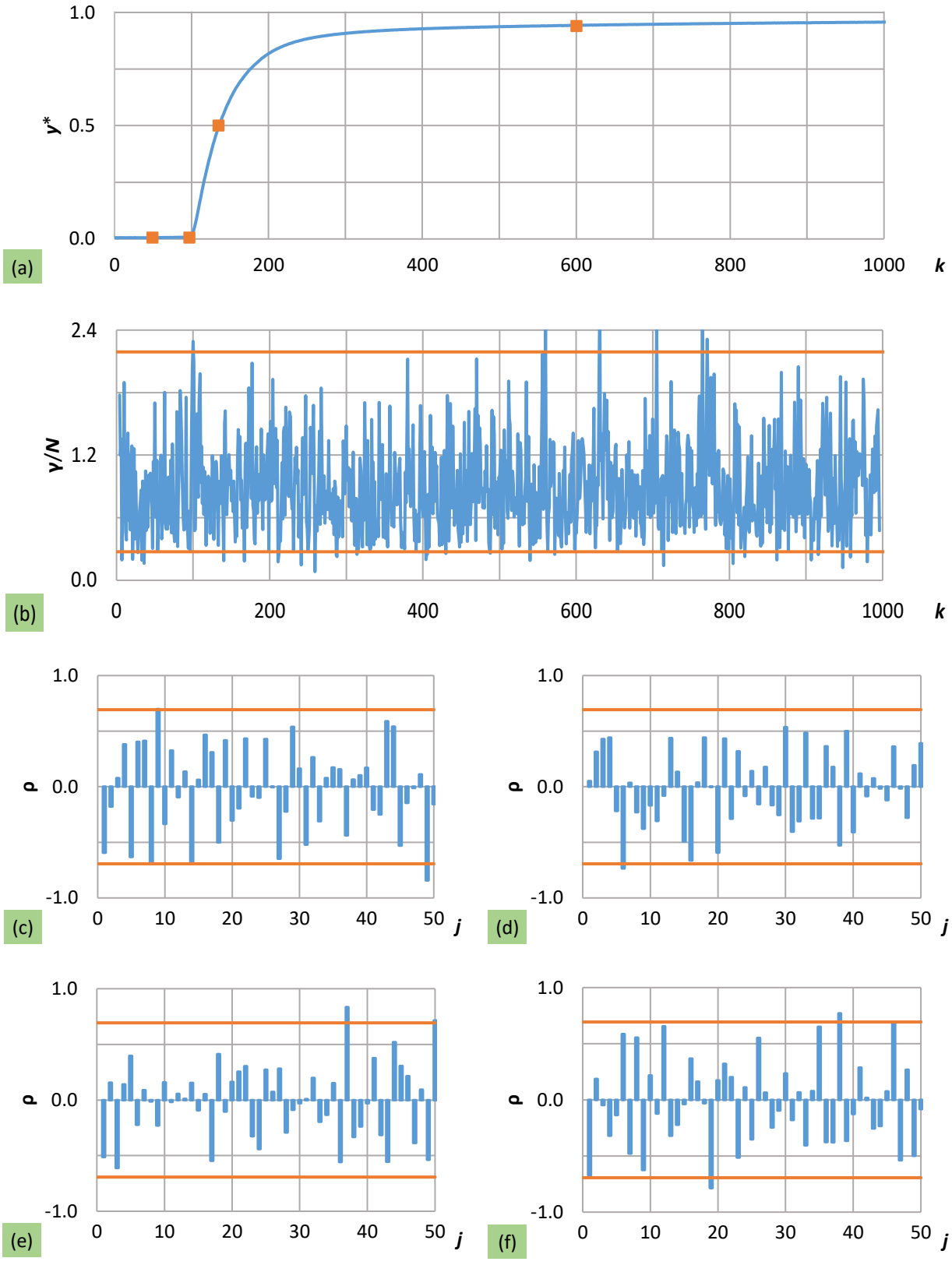

Figure 5. Second-order polynomial model. (a) Mean of normalized sensor step response. (b) Normalized innovation squared test. (c)-(f) Autocorrelation test for different points of the transient response.

This paper presents an approach to solve this problem assuming that the polynomial should keep that part of the information in the signal that makes its estimation possible. The current study establishes that the model of any polynomial in state space is uniquely determined by three hyperparameters: the order of the polynomial model, the intensity of the process noise, and the intensity of the measurement noise. When such a model is part of a Kalman estimation algorithm these parameters can be chosen

after conducting a NIS test and an autocorrelation test by which it is confirmed that the innovation process is white noise (the difference between the measured and the predicted value of the polynomial model is statistically insignificant). The use of polynomial models to represent signals has significant advantages: they have a relatively simple structure and a small number of parameters, they are linear and stationary, they do not require prior information about the observed process and the sensor used (the measurements obtained from the sensor are sufficient to implement the model selection procedure), and they allow real-time operation.

Using the proposed approach, the signal tracking problem of SHT31-DIS humidity sensor is solved, and the second-order polynomial model is found to be quite sufficient to describe the sensor signal. Of course, this does not limit its application and it can be successfully used in many other cases.

References

[1]. Algamili, A. S., Khir, M. H. M., Dennis, J. O., Ahmed, A. Y., Alabsi, S. S., Ba Hashwan, S. S., & Junaid, M. M. (2021). A review of actuation and sensing mechanisms in MEMS-based sensor devices. *Nanoscale research letters*, *16*(1), 1-21.

[2]. Gelen, A. G., & Atasoy, A. (2018, September). A new method for Kalman filter tuning. In *2018 International Conference on Artificial Intelligence and Data Processing (IDAP)* (pp. 1-6). IEEE.

[3]. Saho, K. (2017). Kalman filter for moving object tracking: Performance analysis and filter design. *Kalman Filters-Theory for Advanced Applications*, 233-252.

[4]. Anitha, R., Renuka, S., & Abudhahir, A. (2013, December). Multi sensor data fusion algorithms for target tracking using multiple measurements. In *2013 IEEE international conference on computational intelligence and computing research* (pp. 1-4). IEEE.

[5]. Gan, Q., & Harris, C. J. (2001). Comparison of two measurement fusion methods for Kalman-filter-based multisensor data fusion. *IEEE Transactions on Aerospace and Electronic systems*, *37*(1), 273-279.

[6]. Garcia-Huerta, R. A., González-Jiménez, L. E., & Villalon-Turrubiates, I. E. (2020). Sensor Fusion Algorithm Using a Model-Based Kalman Filter for the Position and Attitude Estimation of Precision Aerial Delivery Systems. *Sensors*, *20*(18), 5227.

[7]. Yufei, L. İ. U., Nogichi, N., & Ishii, K. (2018). Development of a small-sized and low-cost attitude measurement unit for agricultural robot application. *Journal of Agricultural Sciences*, *24*(1), 33-41.

[8]. Isermann, R. (2004). Model-based fault detection and diagnosis-status and applications. *IFAC Proceedings Volumes*, *37*(6), 49-60.

[9]. Khambampati, A. K., Kim, K. Y., Hur, S., Kim, S. J., & Kim, J. T. (2021). An interactive multiple model method to identify the in-vessel phenomenon of a nuclear plant during a severe accident from the outer wall temperature of the reactor vessel. *Nuclear Engineering and Technology*, *53*(2), 532-548.

[10]. He, J., Bai, S., & Wang, X. (2017). An unobtrusive fall detection and alerting system based on Kalman filter and Bayes network classifier. *Sensors*, *17*(6), 1393.

[11]. Christensen, O., & Christensen, K. L. (2004). *Approximation theory: from Taylor polynomials to wavelets*. Springer Science & Business Media.

[12]. Estep, D. J. (2002). *Practical analysis in one variable*. New York: Springer.

[13]. Pinkus, A. (2000). Weierstrass and approximation theory. *Journal of Approximation Theory*, *107*(1), 1-66.

[14]. Mellodge, P. (2015). *A practical approach to dynamical systems for engineers*. Woodhead Publishing.

[15]. Simon, D. (2006). *Optimal state estimation: Kalman, H infinity, and nonlinear approaches*. John Wiley & Sons.

[16]. Grewal, M. S., & Andrews, A. P. (2014). *Kalman filtering: Theory and Practice with MATLAB*. John Wiley & Sons.

[17]. Nikovski Pl., Titova T., Mihov V. (2022). Local polynomial models for real-time tracking of humidity sensor signals. *International Conference on Electronics, Engineering Physics and Earth Science (EEPES 2022).*

[18]. Govaers, F. (Ed.). (2019). *Introduction and Implementations of the Kalman Filter*. BoD–Books on Demand.

[19]. Valade, A., Acco, P., Grabolosa, P., & Fourniols, J. Y. (2017). A study about Kalman filters applied to embedded sensors. *Sensors*, *17*(12), 2810.

[20]. Li, Q., Li, R., Ji, K., & Dai, W. (2015, November). Kalman filter and its application. In *2015 8th International Conference on Intelligent Networks and Intelligent Systems (ICINIS)* (pp. 74-77). IEEE.

[21]. Bar-Shalom, Y., Li, X. R., & Kirubarajan, T. (2004). *Estimation with applications to tracking and navigation: theory algorithms and software*. John Wiley & Sons.

[22]. Nikovski, P. I., Markov, B. G., & Doychinov, N. S. (2019, May). Sampling Time Variation of the EK-H5 Based Humidity Data Acquisition System. In *2019 X National Conference with International Participation (ELECTRONICA)* (pp. 1-3). IEEE.